Available online at www.sciencedirect.com
SCIENCE DIRECT
Polymer 47 (2006) 3401–3409
polymer
www.elsevier.com/locate/polymer

Properties and structure of cyanate ester/polysulfone/organoclay nanocomposites

I. Mondragón [b], L. Solar [a], A. Nohales [a], C.I. Vallo [c], C.M. Gómez [a,*]

[a] *Institut de Ciència dels Materials (ICMUV), Universitat de València, Dr Moliner, 50, 46100 Burjassot, Valencia, Spain*
[b] *Materials+Technology, Escuela Univ. Politécnica. UPV/EHU, Plaza Europa 1, 20018 San Sebastián, Spain*
[c] *Institute of Materials Science and Technology (INTEMA), Universidad Nacional de Mar del Plata-National Research Council (CONICET), Mar del Plata, Argentina*

Received 6 September 2005; received in revised form 10 February 2006; accepted 14 March 2006

Abstract

In this paper, a cyanate ester (CE) matrix has been modified with polysulfone and an organic montmorillonite (Nanofil 919). The blend was thermally cured in presence of copper acetylcetonate and nonylphenol. The morphology of the cured materials was investigated by wide angle X-ray, scanning and transmission electron microscopy techniques. An intercalate structure of silicate platelets in the cyanate matrix has been obtained. Furthermore, results of thermogravimetric analysis (TGA) suggest that CE/PSF/Nanofil 919 nanocomposites have higher thermal stability than the neat resin, increasing the onset decomposition temperature. Flexural strength distributions of modified and neat cyanate matrices were obtained by testing the materials in three-point bending. The results were analyzed within the framework of Weibull statistics. The flexural behavior of the resins demonstrated to be sensitive to the intrinsic flaw distribution. The modified system displayed higher fracture toughness and impact strength compared to pure CE. Dynamic mechanical analysis (DMA) studies confirmed that the PSF modified matrix developed a two-phase morphology consisting of spherical PSF dispersed in a thermoset matrix.

Keywords: Cyanate ester; Clay; Polysulfone

1. Introduction

Cyanate ester resins have been touted as potential replacements for epoxies in high temperature encapsulation applications. These matrices possess great thermal stability, high moisture resistance, low ionic contaminant concentration, good dielectric properties, and have the benefit of being single component materials [1,2]. After heating, the ester monomer undergoes self-cyclotrimerization to form a three-dimensional network structure of polycyanurate [1,2]. For industrial purposes, the cure of these resins is generally carried out in presence of a catalyst system to accelerate the cure process and to attain high levels of conversion [2–4].

However, like most other high performance thermosets, cyanate esters alone do not possess the mechanical properties needed for the applications described above. They can be substantially toughened by the addition of a rubbery or a rigid thermoplastic component [1,2,5–12]. The most effective toughening approach in order to attain an enhancement in fracture toughness has been the incorporation of a high modulus and high glass transition temperature thermoplastic [1,2,6,9–13]. So, the matrix retains its properties such as high modulus and high glass transition temperature. The thermoplastic is initially miscible with the resin and phase separates during polymerization [12–15].

In the last years, the addition of nanoscale fillers, such as layered silicates, has been used as an alternative approach to enhance performance [16–22]. The major reason in introducing these fillers into polymers at the nanoscale level is the pronounced improvements in properties one can obtain at low clay contents. The exfoliated configuration is of particular interest because it maximises the polymer-layered silicate interactions, making the entire surface of the layers available for interactions with the polymer matrix. This should lead to most dramatic changes in mechanical and physical properties.

In order to ascertain the material resistance in flexion, three-point flexure tests utilize rectangular bars subjected to three-point flexural loading, which provides a state of pure tensile stress on the underside of the specimen [23]. It is convenient to

* Corresponding author. Tel.: +34 96 354 4881; fax: +34 96 354 4564.
E-mail address: clara.gomez@uv.es (C.M. Gómez).

0032-3861/$ - see front matter © 2006 Elsevier Ltd. All rights reserved.
doi:10.1016/j.polymer.2006.03.047

determine the flexural strength distribution. So, since these thermoset matrices are brittle materials, the Weibull model [24] can be employed to fit the rupture load distribution.

The objective of the present study is to investigate the possibility to synthesize materials with nanocomposite structure based on a layered organic silicate, a thermoplastic and a cyanate matrix. The material selection has been supported by previous works where polysulfone (PSF)/organo clay and cyanate/organoclay have been studied [16,18,21]. Consequently, the aim of the current study was to investigate the properties and structure of a cyanate matrix modified with PSF and/or an organically modified montmorillonite.

2. Experimental

2.1. Materials

A bisphenol A-based cyanate resin BADCy, (4-4′-dicyanato-2,2′-diphenylpropane) monomer with the trade name of AroCy B10, 99.5% purity and with an equivalent of 139 g/equiv. was gently supplied by Ciba-Geigy. The catalyst system was formed by the complex metal copper (II) acetylacetonate, $Cu(AcAc)_2$, and the co-catalyst nonylphenol, NP, (technical grade) from Aldrich. The thermoplastic used was polysulfone (PSF), (Amoco UDEL P-1700) with M_w/M_n: 38,000/36,000 and $T_g = 185$ °C. The layered silicate used in this study is an industrial organically modified montmorillonite with commercial trade name Nanofil 919 supplied by Süd Chemie. It has a cation exchange capacity (CEC) of 0.75 mmol/g being the Na^+ ions substituted by sterylbenzyldimethylammonium chloride, $(CH_3)_2N^+CH_2PhHT$ where HT is 65% C18, 30% C16 and 5% C14. The medium particle size is 35 M, it shows a loss of ignition of 35 wt% and an interlaminar distance of 1.91 nm.

2.2. Sample preparation

Cyanate resin was blended with the required amount of the catalytic system, that is, $Cu(AcAc)_2$ at concentration of 360 ppm and NP at a concentration of 2% of the total resin weight (phr), prior to cure. The required amount of metal catalyst was predissolved in NP at 100 °C with continuous stirring until a homogeneous mixture was obtained and cooled down to room temperature. The catalytic blend was added to the preselected weight of the molten resin at 90 °C, stirred for 5 min to obtain a homogeneous mixture and immediately quenched before any reaction could occur. Prior to cure, the catalysed samples were stored in the refrigerator in a desiccator to avoid moisture absorption. The organoclay was previously dried for 24 h at 80 °C and mixed with the resin for 30 min at room temperature using a high-shear mixing blade Dispermat® CN20 (VMA-Getzmann GMBH, Alemania) at 7100 rpm with a 5-cm-diameter disk for 25 min. The PSF-Nanofil modified cyanate was prepared by adding 10 wt% PSF to the previous cyanate/Nanofil mixture at 90 °C. Air bubbles introduced during stirring were removed keeping the sample under vacuum at 90 °C for a short period of time.

Plates were obtained by casting the mixtures into moulds consisting of two rectangular glass plaques covered with Freetoke release agent spaced by a 5 mm Teflon frame and held together with clamps. The cure schedule was 3 h at 170 °C, 2 h at 200 °C and 1 h at 250 °C. A DSC analysis of the samples confirmed that they were fully cured. The cured plaques were allowed to cool slowly to room temperature, removed from the mould and machined to produce bars for mechanical testing.

2.3. Characterization

X-ray diffraction patterns (XRD) were recorded on a Seifert analytical X-ray 3003 TT X-ray diffractometer using the Cu K_α radiation.

The morphology of the PSF and/or Nanofil 919 cyanate resin was studied by scanning electron microscopy (SEM) and by transmission electron microscopy (TEM). The scanning electron microscope was a Hitachi S-4100 with an acceleration of 10 kV and a distance around 12–14 mm. Samples for SEM observations were fractured in liquid nitrogen. The specimens for transmission electron microscopy were prepared by microtoming in a Reichert-Jung Ultracut Microtome at room temperature and inspected using a transmission electron microscope (TEM) model Jeol Jem-1010 Electron Microscope.

The thermal gravimetric curves were measured on a Setaram Setsys 92-12 under argon flow. The temperature range was 25–1000 °C with a heating rate of 10 °C/min. The temperature was determined with a commercially thermocouple type S noble-metal (Pt/Pt Rh (10%)) that can be used up to about 2000 °C with an error of 0.28%. The error bar in mass measurements was ± 0.4 μg.

The unmodified and PSF and/or Nanofil 919 modified cyanate polymers were tested under flexure using the three-point bending test experiment according to ASTM D790-93 [25] protocol. An Instron 5582 Universal Tester equipped with a 5 kN load cell at (23 ± 2) °C was used at a crosshead displacement rate of 5 mm/min. The specimen dimensions were equal to (5 ± 0.1) mm × (10 ± 0.2) mm crosssection and (100 ± 5) mm in length. The length between supports was 80 mm as recommended by the protocol.

The flexural strength (σ_f), the maximum strain in the outer fibre (ε) and the flexural modulus (E) were calculated from the following expressions by loading the bars to failure

$$\sigma_f = \frac{3PL}{2bd^2}\left[1 + 6\left(\frac{\delta}{L}\right)^2 - 4\left(\frac{\delta d}{L^2}\right)\right] \quad (1)$$

$$\varepsilon = \frac{6\delta d}{L^2} \quad (2)$$

$$E = \frac{L^3 s}{4bd^3} \quad (3)$$

where P is the load at break, b and d are the width and the thickness of the specimen, L is the length between supports, δ is the maximum deflection of the centre of the beam and s is the slope of the tangent to the initial straight-line portion of

the load-deflection curve. According to the ASTM protocol, Eq. (1) has been used in this paper since the maximum outer-fibre strain, ε, exceeds 5% before fracture.

Fracture toughness experiments were conducted using a single edge notched bend specimens according to ASTM E-399 protocol at (23±2) °C and crosshead displacement rate of 1.6 mm/min. The specimen dimensions were equal to (5±0.1) mm×(10±0.2) mm crosssection and (50±5) mm in length. The length between supports was 40 mm. A minimum of five specimens were used.

The critical stress intensity factor, K_{IC} was calculated using the following expression

$$K_{IC} = \left(\frac{P}{Bw^{1/2}}\right) f(x) \tag{4}$$

where, w is the sample width, B is the specimen thickness and $f(x)$ is a mathematic function that depends on crack length and the sample width.

Then, the critical strain energy release rate, G_{IC}, can be calculated by using the following expression

$$G_{IC} = \frac{(1-\nu^2)K_{IC}^2}{E} \tag{5}$$

where, ν is the Poisson coefficient taken as 0.35 [26].

Dynamic mechanical analysis (DMA) tests were performed on a 2980 Dynamic Mechanic Analyzer (TA instruments) in the three point bending mode at a frequency of 1 Hz and amplitude of 30 μm over the temperature range 30–350 °C. The heating rate was 3 °C/min. Samples used were rectangular strips with dimensions (50×12×5) mm. The storage modulus (E') and the damping factor (tan δ), as a measurement of the glass transition temperature (T_g), were recorded.

3. Results and discussion

3.1. Morphological characterization

In this study, microcomposites have been formed by incompatibility between polysulfone and the build up of a crosslinked cyanate network, whereas, nanocomposites have been formed via diffusion of the oligomeric prepolymer into the interlayer regions, followed by crosslinking. The morphology of these nano and/or micro composites was studied using the XRD patterns, TEM and SEM observations.

Fig. 1 shows XRD profiles of dried Nanofil (a), (b) CE/2 wt% Nanofil and (c) CE/2 wt% Nanofil/10 wt% PSF. Nanofil has an interlayer spacing (d_{001}) of 1.91 nm corresponding to a diffraction peak angle, $2\theta = 4.64°$. After the curing process was completed, this interlayer spacing shifts to 3.88 nm ($2\theta = 2.49°$) for Nanofil/cyanate, very close to the value obtained in presence of PSF ($d_{001} = 3.94$ nm, $2\theta = 2.27°$), which is indicative of a certain degree of mass transfer into the galleries. Similar shifts have been observed [16,18] for epoxy and cyanate systems indicating intercalation of cyanate into the clay, as well as for PSF/organoclay systems [21].

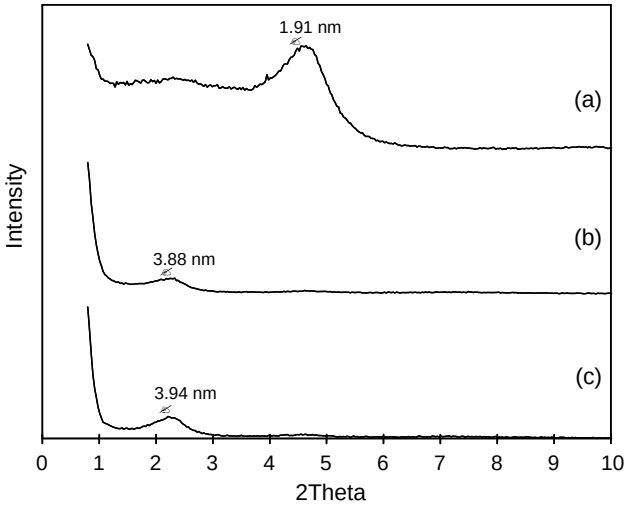

Fig. 1. X-ray diffraction patterns of (a) Nanofil, (b) CE/2 wt% Nanofil and (c) CE/2 wt% Nanofil/10 wt% PSF.

Fig. 2 shows the surface of the different systems as observed by scanning electron microscopy (SEM), that is, the unmodified resin (a), 2 wt% Nanofil (b), 10 wt% PSF/2 wt% Nanofil (c) and 10 wt% PSF (d) modified resin. The PSF modified resin prepared as described was homogeneous, clear and transparent, at the early stage of reaction (similar to the neat resin). As the polymerization reaction proceeded, the system developed a two-phase morphology due to two competing factors, phase separation and matrix polymerization, resulting in an opaque system. As can be observed in Fig. 2(c) and (d) the PSF has been segregated from the cyanate matrix as spherical domains originated during the course of polymerisation with a certain degree of adhesion between the matrix and the thermoplastic. Spherical particles of approximately 0.3 μm corresponding to the PSF phase dispersed in

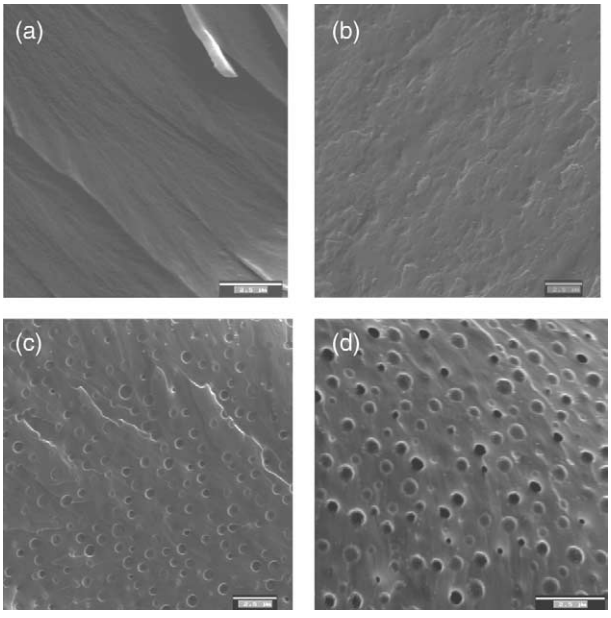

Fig. 2. SEM micrographs of (a) neat cyanate, (b) CE/2 wt% Nanofil, (c) CE/2 wt% Nanofil/10 wt% PSF and (d) CE/10 wt% PSF.

the cyanate rich matrix are observed. In turn, the Nanofil modified cyanate resin shows a rough surface (Fig. 2(b)), whereas, the CE/Nanofil/PSF (Fig. 2(c)) depicts a similar two phases structure to Fig. 2(d) from the micro scale point of view. It is widely recognized that in order to achieve good toughening in a thermoplastic modified cyanate system, adequate interfacial adhesion is necessary. The fracture surface of modified cyanate shows coarse feature due to fast fracture. Visual examination of the fracture surfaces of the unmodified resin revealed that the crack showed flat propagation with a very smooth 'mirror like' zone, which is characteristic of brittle crack propagation. Conversely, the fracture surface of the thermoplastic/organoclay modified resins, presented a rougher aspect compared with the neat resin. The crack spreads regularly and oriented in the direction of loading, suggesting typical characteristics of brittle fracture. The behaviour observed when testing the material under fracture can be attributed to the relatively low elongation of the PSF at failure and the limited ability of the brittle matrix to undergo shear deformation.

The intercalated structure in the Nanofil systems is further supported by TEM micrographs presented in Fig. 3. No exfoliated clay platelets are observed, whereas, small stacks of intercalated Nanofil are randomly distributed in the cyanate matrix. As it is frequently the case, the layers appear to be roughly parallel to one another [27]. Van der Waals and Coulombic forces between intergalleries are so strong that the silicate layers cannot be easily separated. Whether it is exfoliated individually or merely intercalated is determined by the above two forces and the force between monocyanate and organoclay surface. Besides, the nano-scale organoclay layers have high specific surface area and surface energy, which also makes them to aggregate together rather than to disperse homogeneously in the continuous cyanate matrix. Nanometer-range intercalated clay tactoids can be clearly seen in Fig. 3(b) and (d). The dark lines correspond to the crosssection of the clay sheets of ca. 1 nm thickness and the gap between two adjacent lines is the interlayer spacing or gallery. The measured distance between the two adjacent lines, i.e. the interlayer spacing of the intercalated tactoids, obtained from TEM observations, is consistent with those from the XRD data. In Fig. 3(c), we can observe 0.3–0.4 μm diameter spherical PSF particles homogeneously dispersed in the matrix without any silicate layer intercalated. Presumably, the interaction clay/cyanate is higher than clay/PSF under the experimental conditions followed to cast the plaques in this work. Nanofil has been dispersed in excess of cyanate and some resin has been situated between the silicate platelets. There could also be a kinetic complication specifically the relatively small entropic driving force for additional randomization not being sufficient to immediately overcome the high viscosity of the medium due to PSF phase separation upon the increase of cyanate molecular weight. So not intercalation between PSF and Nanofil has been

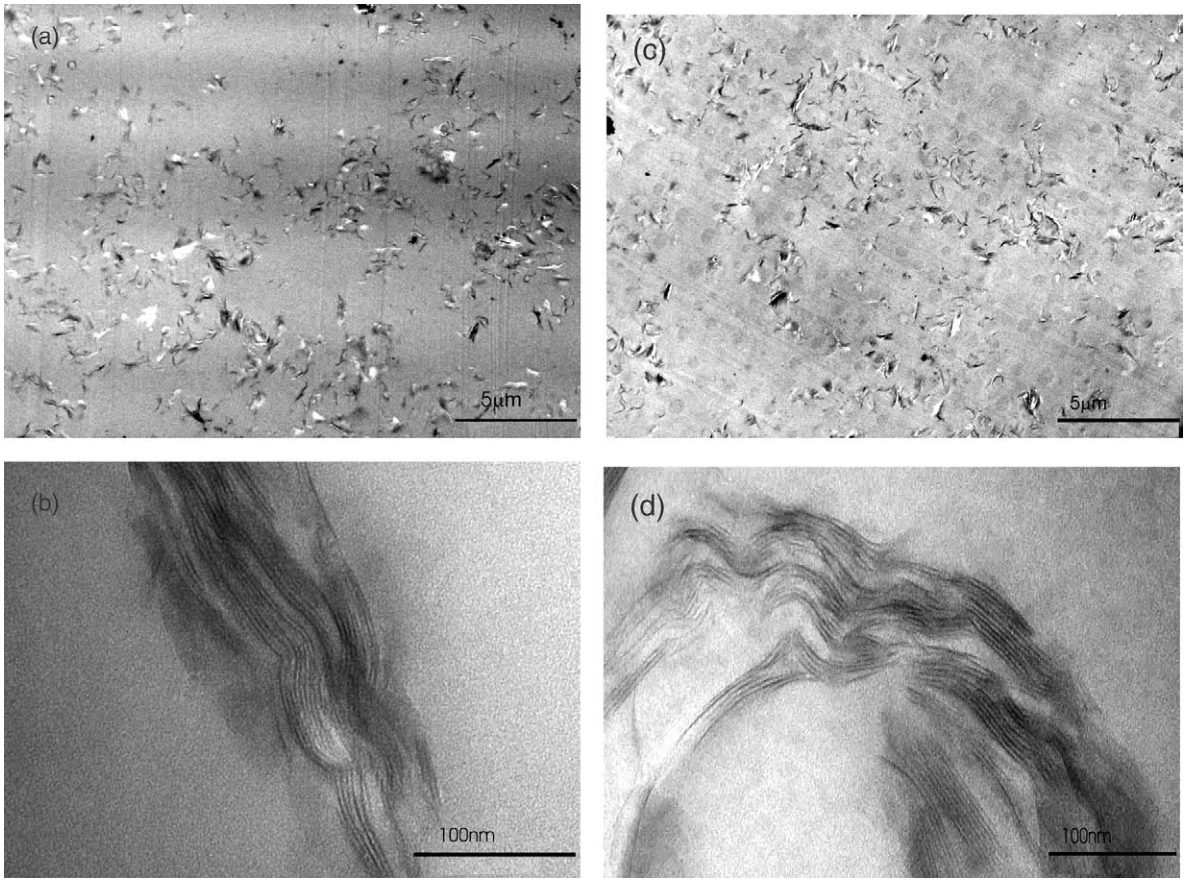

Fig. 3. Transmission electron images of the nanocomposites. (a, b) CE/2 wt% Nanofil and (c, d) CE/2 wt% Nanofil/10 wt% PSF.

detected upon the weight ratio investigated and experimental conditions employed, similar to a published study [21].

3.2. Thermo stability of composites

Fig. 4 shows the thermogravimetric curves (a) (TG curves) and corresponding derivative curves (b) (DTG curves) for unmodified and PSF/Nanofil modified resin. The initial thermal decomposition temperatures (onset temperature) of unmodified resin, CE/10 wt% PSF, CE/2 wt% Nanofil and CE/10 wt% PSF/2 wt% Nanofil and nanocomposites are 408, 422, 417 and 420 °C, respectively. This is possibly due to thermoxidative degradation of the ether oxygen bond between the phenyl and triazine rings [2]. The onset temperature decomposition of the nano/micro composites is higher than for the neat matrix. This may result from the interaction between organic and inorganic phases and copolimerization between cyanate ester and Nanofil ($NH_4^+ - MMT$). This may be partly due to kinetic effects, with the platelets of organosilicate and spherical particles of PSF retarding decomposition of the polymer matrix. These results indicate that modified cyanate resin has better thermal stability than the neat resin. Similar results of higher thermal decomposition temperature of intercalated CE/organoclay nanocomposites have been reported [16,18]. There are two peak temperatures in the typical DTG thermograms for all samples as shown in Fig. 4(B). The first maximum decomposition rate temperatures for the unmodified resin, CE/10 w% PSF, CE/2 wt% Nanofil and CE/10 wt% PSF/2 wt% Nanofil nanocomposites were 436, 433, 433 and 435 °C, respectively. They correspond to thermo decomposition of the ether oxygen bond between the phenyl and triazine rings. In fact, this first peak is not influenced by the addition of organic/inorganic modifiers. The second decomposition is due to the breakdown of the triazine ring and the peak appears at 505 °C for unmodified resin, 507 and 509 °C for CE/2%wt Nanofil and PSF/2 wt% Nanofil, respectively, and 511 °C for CE/10 wt% PSF, indicating a slight improvement for the PSF modified cyanate resin.

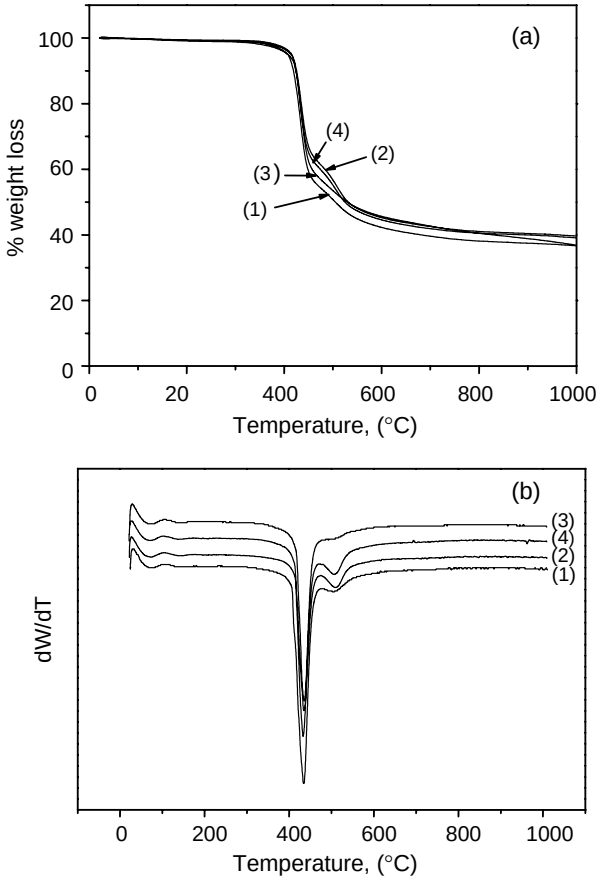

Fig. 4. Thermogravimetric (a) and differential thermogravimetric (b) curves of: (1) neat cyanate, (2) CE/10 wt% PSF, (3) CE/2 wt% Nanofil and (4) CE/2 wt% Nanofil/10 wt% PSF.

3.3. Flexural test

Much of the work concerning the mechanical characterization of unmodified and thermoplastic/organoclay modified resins has been performed by testing the materials under flexure [28–32]. This may be attributed to the fact that, in the case of brittle materials subjected to tensile test, a slight misalignment of the axial load is sufficient to cause premature failure at the grips.

Three-point bending tests were carried out for the unmodified and modified cyanate resin. Load–deflection curves were plotted to determine the flexural strength, the tangent modulus of elasticity and the strain at break. Fig. 5 shows a representative plot of load versus deformation obtained in bending tests. Rupture loads of brittle materials usually result in high data scatter, hence, in order to analyse the flexural strength data distribution a number of specimens higher than that recommended by the ASTM D790 protocol has to be tested. As a compromise between minimizing both the dispersion of the evaluation method and the experimental effort, the use of a minimum number of 15 specimens has been suggested [33–36]. In the present work, 20 and 18 specimens for the unmodified and modified cyanate resin, respectively, have been tested.

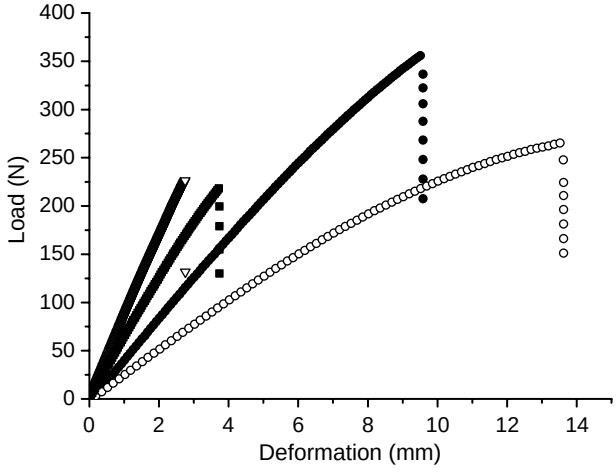

Fig. 5. Load versus displacement curves for the different systems assayed: (●) neat resin, (○) 9 CE/10 wt% PSF, (▽) CE/2 wt% Nanofil, (■) CE/10 wt% PSF/2 wt% Nanofil.

Flexural strength data were analysed within the frame of Weibull statistics, which is the most widely used expression for mechanical characterisation of brittle materials. The Weibull model links the failure probability of a piece, P_f, to the rupture stress, σ_f, by means of the relation

$$P_f = 1 - \exp\left[-\left(\frac{\sigma_f}{\sigma_0}\right)^m\right] \quad (6)$$

P_f is the cumulative fracture probability for the stress σ_f, m is the Weibull modulus and σ_0 is a scale parameter. The Weibull modulus, m, is a material parameter which characterizes the scattering in the measured values of strength. The higher the m value, the less the data scatter. The mean flexural strength is calculated from the following expression

$$\sigma_m = \sigma_0 \Gamma\left(1 + \frac{1}{m}\right) \quad (7)$$

where Γ is the gamma function.

Different methods have been used for the evaluation of Weibull parameters [24,25,28–30]. The most common method has been the linear least squares method applied to the linearized form of Eq. (6)

$$\ln \ln\left[\frac{1}{1-P_f}\right] = m \ln \sigma_f - m \ln \sigma_0 \quad (8)$$

the value of P_f for each σ_f was estimated using the following estimator [35]

$$P_i = \frac{i - 0.5}{N} \quad (9)$$

where i is the rank number of the flexural strength and N is the number of samples.

Table 1 compiles the rupture loads values measured for the systems tested. The results were ordered from the lowest stress to rupture to the highest and the probability of failure, P_f, was calculated by the estimator given in Eq. (9). Fig. 6 depicts the Weibull plots for the unmodified and modified cyanate resin. The two parameters m and σ_0, knowledge of which leads to the complete characterisation of the material, were determined from the slope and from the ordinate at the origin of the linear representation given in Fig. 6. The degree of fit to the two-parameters Weibull model was determined by how well the data group around a straight line (Eq. (8)). Satisfactory agreement is observed between the experimental results and the Weibull equation. Cumulative distributions of failure probability, P_f versus σ_f calculated after the estimation of the Weibull parameters from Eq. (6) are shown in Fig. 7.

Table 1
Flexural strength results measured for the systems under study

i	σ_f (MPa) CE	σ_f (MPa) PSF/CE	σ_f (MPa) PSF/ Nanofil/CE	σ_f (MPa) Nanofil/CE
1	91.5	120.2	71.8	66.2
2	92.0	120.6	78.1	74.1
3	98.8	121.0	80.9	81.1
4	103.0	123.0	82.3	83.1
5	110.4	124.3	84.9	85.9
6	115.9	129.7	86.8	89.0
7	122.6	132.4	87.3	90.1
8	124.3	134.3	89.7	92.1
9	126.8	135.8	90.3	100.7
10	127.1	136.1	91.9	101.8
11	129.6	138.0	94.1	105.5
12	130.1	139.0	97.1	106.1
13	135.3	139.3	99.4	107.7
14	138.3	141.6	100.0	111.8
15	138.6	142.9	102.3	113.6
16	140.4	148.1	103.2	114.9
17	141.9	149.9	103.9	116.4
18	143.9	154	105.8	117.6
19	145.8			
20	152.3			

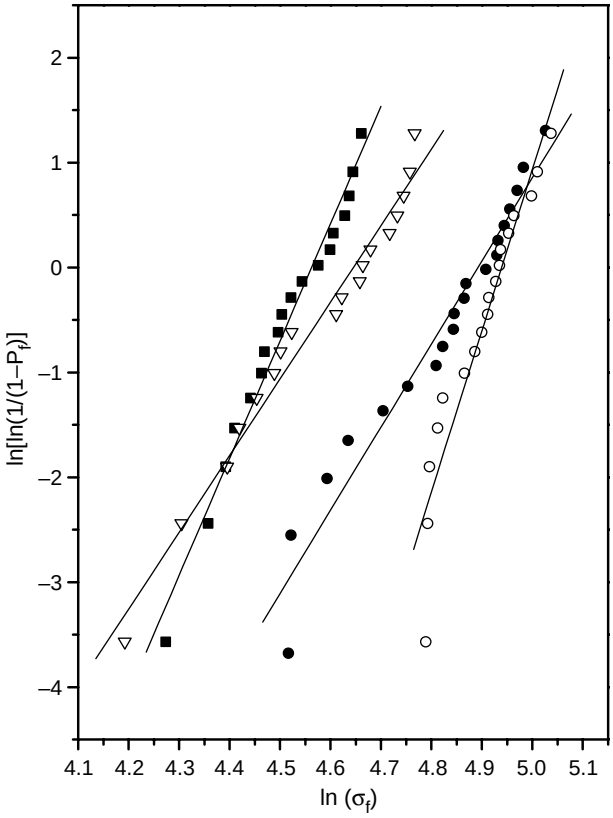

Fig. 6. Weibull plots for the systems under study (●) neat CE; (○) CE/10 wt% PSF; (▽) CE/2 wt% Nanofil and (■) CE/10 wt% PSF/2 wt% Nanofil.

Results of the mean flexural properties are shown in Table 2. The Weibull modulus, m, characterizes the scattering in the measured values of strength. The higher the m value, the less the data scatter. From the m values presented in Table 2, it emerges that the addition of thermoplastic resulted in a markedly reduced data scatter of the flexural strength data. On the other hand, it can be seen that the flexural modulus was not significantly changed by the thermoplastic and/or organoclay modification. Flexural strength was slightly improved by the incorporation of the thermoplastic modifier, nevertheless the addition of Nanofil reduced its value.

The Mann–Whitney test comparison of the mean flexural strength for the unmodified and thermoplastic/organoclay modified resins indicates that, at the 95% confidence level, the means are not significantly different. However, two

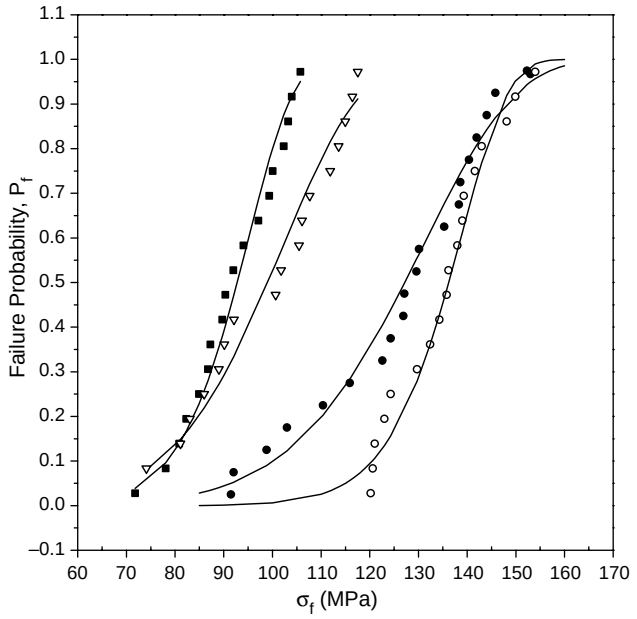

Fig. 7. Weibull cumulative strength distribution for (●) neat CE; (○) CE/10 wt% PSF; (▽) CE/2 wt% Nanofil and (■) CE/10 wt% PSF/2 wt% Nanofil.

different materials with similar mean flexural strength values might have very different distributions of the data points. In this case, the material with the larger data spread would have more weak specimens and, thus, would probably have a greater incidence of failure. From the Weibull distribution it is possible to compare the failure probabilities at a given strength level. The comparison of the percentage of specimens broken at a certain load level demonstrates that the unmodified resin and Nanofil 919 modified resin had a higher number of weak specimens. For example, at a load of 130 MPa, for PSF modified resin the percentage of specimens broken was 33% while for the unmodified resin was 60%. This marked difference is a consequence of the higher data scatter of the unmodified and Nanofil modified resin compared with the thermoplastic modified resin.

The critical stress intensity factor, K_{IC} and critical strain energy release rate, G_{IC}, results are shown in Table 3. The critical stress intensity factor slightly increases in modified systems. It is generally accepted that such increase is primarily a result of an increase in crack front pinning/blunting efficiency due to smaller interparticle distances [37]. The addition of the organoclay to cyanate ester resin also improves impact strength, comparing with the neat resin. Fracture energies were calculated using values on fracture toughness and flexural modulus reported in Section 3.2. The PSF modified system shows the higher value of G_{IC}, 347 J m^{-2} compared with unmodified system, 165 J m^{-2}. The improvement of this property is probably due to the good adhesion of PSF particles in the cyanate matrix how we can observe in SEM photographs. The addition of 2 wt% Nanofil to neat resin causes a lower improve of G_{IC} compared to the addition of 10 wt% PSF. Probably, the addition of more quantity of organoclay with a better dispersion leading to complete exfoliation of the organoclay in the matrix will enhance the fracture energy. The intercalated/exfoliated dispersion of the organosilicate layers into the matrix will determine the improvement in the mechanical properties compared with unmodified system [22].

Polymer/layered silicate nanocomposites have been studied as a new generation of polymeric materials. Wang et al. [38] developed a process for the incorporation of clay to an epoxy matrix. Clay was highly exfoliated into thin tactoids which dispersed uniformly and oriented randomly in the epoxy matrix. The authors found that both Young's modulus and fracture toughness were markedly improved by the addition of 2.5 wt% of clay. On the contrary, epoxy nanocompoaites in which the dispersion of organoclay was poor and the filler formed aggregates of about 10–20 μm in size resulted in a decreased tensile strength compared with the neat epoxy resin. These results are in agreement with the bending tests results observed in the present work, and reveal the influence of the resulting microstructure of the nanocomposites on the mechanical properties.

Dynamic mechanical data (storage modulus, E', and tan δ) for the systems studied are depicted in Fig. 8. The unmodified resin displays a single loss peak corresponding to its glass transition temperature, $T_g = 298$ °C. The tan δ traces of the PSF modified matrices exhibited two relaxation peaks, confirming the development of a phase-separated morphology. The higher temperature relaxation is associated with the T_g of the cyanate-rich phase and the lower with the T_g of the PSF. The area of the higher temperature peak of modified systems diminished considerably compared with the area of the peak of unmodified system, indicating that the addition of PSF or Nanofil influences the polymerization of the resin. These results are similar to clay/epoxy nanocomposites [37]. Either increased glass transition temperatures [16] or a constant or slightly decreased [37] T_g values have been reported for themoset nanocomposites. In general, the increase in T_g is attributed to the good adhesion between the polymer and the reinforced particles so that the nanometer size particles can restrict the segmental motion of crosslinks under loading. The other important factors that can affect T_g are degree of particle dispersion and curing conditions. The degree of particle dispersion includes size, homogeneity, orientation and spacing

Table 2
Flexural strength (σ_f), Weibull modulus (m) (Eq. (7)), deformation at break (ε) and flexural modulus (E) and mean flexural strength (Eq. (8)) for the different systems

System	σ_f (MPa)	m	ε (%)	E (GPa)	σ_m (MPa)
Unmodified	125.4	7.9	5.13 (0.75)	3.13 (0.08)	125.1
PSF /CE	135.0	15.4	6.66 (0.76)	3.02 (0.16)	134.7
PSF/Nanofil/CE	91.6	11.2	2.96 (0.29)	3.11 (0.14)	91.5
Nanofil/CE	97.7	7.3	3.27 (0.61)	3.21 (0.07)	97.6

Table 3
Fracture toughness, K_{IC} and fracture energy, G_{IC} for the systems investigated

Material	K_{IC} (MPa m$^{1/2}$)	G_{IC} (J m^{-2})
Unmodified	0.76±0.08	165.1±13
PSF/CE	1.08±0.15	347.4±16
PSF/Nanofil/CE	0.89±0.19	237.6±20
Nanofil/CE	0.92±0.12	238.3±18

between particles, whereas, curing conditions include curing speed and degree of crosslinking. The small decrease in T_g observed in this study may arise from some of these factors. Since T_g decreases indicates that it is not an 'adsorbed layer' effect as this usually increases the glass transition temperature due to chains being tied down by the surface of the silicate. It has been found [39] that the T_g of intercalated polymers shows a reduced value due to the lack of surroundings entanglements as characterized by solid-state NMR.

4. Conclusions

A cyanate matrix was modified by the incorporation of an organically modified layered silicate (Nanofil 919) and/or polysulfone (PSF). An intercalated structure of the organoclay has been attained as observed from wide-angle X-ray and transmission electron analysis. The PSF is initially miscible with the cyanate pre-polymer and phase separates in spherical microdomains during the course of cyanate polymerization without severe reduction on the flexural modulus. Thermogravimetric analyses indicate improved thermal stability for the modified matrices respect the onset decomposition temperature. The flexural modulus was not significantly modified by the thermoplastic/organoclay modification. Flexural strength was slightly improved by the incorporation of the thermoplastic modifier; nevertheless the addition of Nanofil 919 reduced the value. Fracture toughness, K_{IC} and fracture energy, G_{IC}, of the cyanate resin were slightly improved by the addition of PSF and Nanofil 919. These improvements are attributed to the good adhesion level of PSF particles to the matrix as well as the homogeneously dispersion of organosilicate layers into the system.

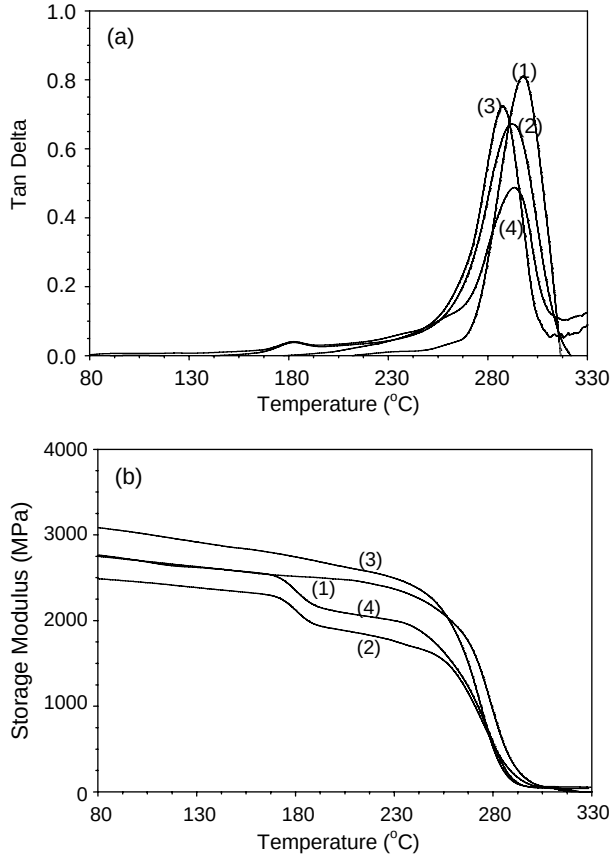

Fig. 8. Tan δ (a) and storage modulus (b) for the unmodified (1), PSF modified (2), Nanofil (3) and PSF/Nanofil (4) modified cyanate matrix.

Acknowledgements

We are grateful for the financial support under contract MAT2002-03485 from Ministerio de Ciencia y Tecnologia (Spain). L. Solar is also indebted for a FPI fellowship grant.

References

[1] Nai CP, Mathew D, Ninan KN. Adv Polym Sci 2001;155:1–99.
[2] Hamerton I. Chemistry and technology of ester resins. Glasgow: Blackie Academic and Professional; 1994.
[3] Bartolomeo P, Chailan JF, Vernet JL. Eur Polym J 2001;37:659–70.
[4] Mathew D, Nair CPR, Ninan KN. J Polym Sci, Part A: Polym Chem 1999; 37:1103–14.
[5] Pascault J-P, Sautereau H, Verdu J, Williams RJJ. Thermosetting polymer. New York: Marcel Dekker, Inc.; 2002.
[6] Paul CR, Bucknall CB, editors. Polymer blends, vol. 2. New York: Wiley; 2000.
[7] Harismendy I, Del RM, Valea A, Gavalda J, Mondragón I. J Appl Polym Sci 2002;83:1799–809.
[8] Cao Z, Mechin F, Pascault J-P. Polym Int 1994;34:41–8.
[9] Srinivasan SA, McGrath JE. Polymer 1998;39:2415–27.
[10] Kim YS, Kim SC. Macromolecules 1999;32:2334–40.
[11] Hedrick JL, Yilgor I, Jurek M, Hedrick JC, Wilkes GL, McGrath JE. Polymer 1991;32:2020–32.
[12] Hwang JW, Park SD, Cho K, Kim JK, Park CE, Oh TS. Polymer 1997;38: 1835–43.
[13] Woo EM, Shimp DA, Seferis JC. Polymer 1994;35:1658–65.
[14] Hwang JW, Cho K, Park CE, Huh W. J Appl Polym Sci 1999;74:33–45.
[15] Woo EM, Su ChC, Kuo J-F, Seferis JC. Macromolecules 1994;27: 5291–6.
[16] Ganguli S, Dean D, Jordan K, Price G, Vaia R. Polymer 2003;44:1315–9.
[17] Pinnavaia TJ, Beall GW, editors. Polymer–clay nanocomposites. New York: Wiley; 2000.
[18] Feng Y, Fang Z, Mao W, Gu A. J Appl Polym Sci 2005;96:632–7.
[19] Kornmann X, Lindberg H, Berglund LA. Polymer 2001;42:4493–9.
[20] Lan T, Kaviratna PD, Pinnavaia TJ. Chem Mater 1995;7:2144–50.
[21] Sur GC, Sun HL, Lyu SG, Mark JE. Polymer 2001;42:9783–9.
[22] Wooster TJ, Abrol S, Hey JM, MacFarlane DR. Macromol Mater Eng 2004;289:872–9.
[23] Darwell BW. J Mater Sci 1990;25:757–80.
[24] Weibull W. J Appl Mech 1951;18:293–7.
[25] ASTM SpecificationD790-93. Flexural properties of unreinforced and reinforced plastics and electrical insulating materials Annual Book of ASTM Standards.
[26] Spanoudakis J, Young RJ. J Mater Sci 1984;19:374.
[27] Wang Z, Pinnavaia T. J Chem Mater 1998;10:1820.

[28] Min BG, Hodgkin ZH, Stachursky ZH. J Appl Polym Sci 1993;50:1063–5.
[29] Min BG, Stachursky ZH, Hodgkin JH. J Appl Polym Sci 1993;50:1511–8.
[30] Di PG, Motta O, Recca A, Carter JT, McGrail PT, Acierno D. Polymer 1997;38:4345–8.
[31] Huang P, Zheng S, Huang J, Guo Q. Polymer 1997;38:5565–71.
[32] Mackinnon AJ, Jenkins SD, McGrail PT, Pethrick RA. Polymer 1993;34: 3252–63.
[33] Khalili K, Kromp J. Mater Sci 1991;26:6741–52.
[34] Peterlik HJ. Mater Sci 1995;30:1972–6.
[35] Riccardi CC, Vallo CI. Polym Eng Sci 2002;42:1260–73.
[36] Vallo CI. Polym Test 2002;21:793–800.
[37] Becker O, Varley R, Simon G. Polymer 2002;43:4365–73.
[38] Wang K, Chen L, Wu J, Toh ML, He C, Yee A. Macromolecules 2005;38: 788–800.
[39] Zax D, Yang D, Santos R, Hegemann H, Giannelis H, Manias E. J Chem Phys 2000;112(6):1951–2945.